15th AIAA/CEAS Aeroacoustics Conference (30th AIAA Aeroacoustics Conference)
11 - 13 May 2009, Miami, Florida

AIAA 2009-3357

LES of noise induced by flow through a double diaphragm system

Alois Sengissen & Bastien Caruelle *
AIRBUS, Toulouse, France

Pascal Souchotte & Emmanuel Jondeau †
LMFA, Écully, France

Thierry Poinsot ‡§
CERFACS & IMFT, Toulouse, France

This paper aims at predicting the noise generated in internal flows using unstructured LES. A canonical geometry representative of complex air conditionning system parts is selected to perform extensive validation of the numerical approach. An experimental campaign carried out at LMFA provides both detailed aerodynamic description of the flow and the wall pressure spectra. The impact of important numerical parameters such as numerical scheme and boundary conditions is then investigated, before assessing the ability of the method to capture physical trends between two similar configurations.

I. Introduction

Large Eddy Simulation (LES) is a promising tool for Computational Fluid Dynamics (CFD) and Computational AeroAcoustics (CAA) purposes. Many research programs have demonstrated the ability of this approach to capture the noise induced by various external flows such as jets,[1,2] shear layers[3,4] or flows around high lift devices.[5,6] A common point of all of these simulations is the use of high order centered numerical schemes on multi-bloc structured grids.[7,8]

In the case of internal flows, the generation of structured meshes of complex geometries such as parts of cockpit's air conditioning system ducts (Fig. 1) is a serious issue. Unstructured/hybrid grids are a possible alternative but building higher order schemes (6^{th} order or more) is a very difficult task due to the limited stencil. This is probably one of the main reasons why the number of aeroacoustic studies using unstructured meshes are very limited.[9] The challenging question is: what can be expected from an unstructured code using a classical 2^{nd} order centered scheme and how significant is the improvement of the results when a state-of-the-art 3^{rd} order scheme is employed ?

These investigations have been performed on a flow through a canonical double diaphragm system previously published[10–12] (described in section II), where a strong aeroacoustic resonance is susceptible to occur or not, depending on the distance L between the diaphragms.

The first objective of this paper is to evaluate the ability of an unstructured LES code (section III) to capture the noise generating mechanisms and to yield accurate noise spectra. The issue at stake is the prediction of trends between designs within reasonable industrial turnover times (64CPU - 100h). This strong constraint must be kept in mind in the perspective of future application on aircraft systems. A second objective is to analyze the influence of several numerical parameters on the aeroacoustic simulation such as boundary conditions' impedance or subgrid model. The simulations will be compared with detailed experimental database (section IV) in terms of mean and fluctuating velocity profiles and wall pressure spectra (section V).

*AIRBUS France, 316 route de bayonne, 31060 Toulouse cedex, France
†LMFA, 36 avenue Guy-de-Collongue, 69134 Écully cedex, France
‡CERFACS, 42 Avenue G. Coriolis, 31057 Toulouse cedex, France
§IMFT, Avenue C. Soula, 31400 Toulouse, France

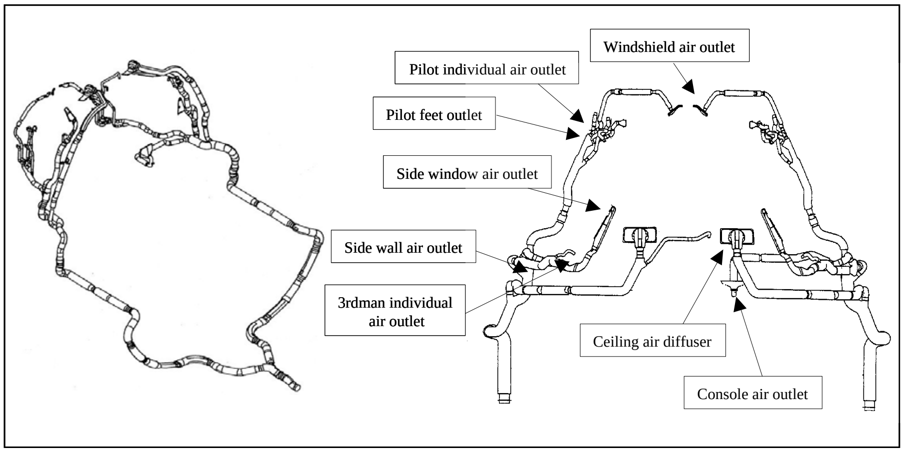

Figure 1. Illustration of typical cockpit air conditionning system network

II. Investigated configuration

Acoustic tones resulting from various types of flows are particularly perceivable when emerging from background broadband noise. Air conditioning systems are very complex in terms of geometry and flows where resonances may occur. Even if the simpler configuration studied here is not present in any air conditionning system, it is representative of such undesirable resonance phenomena and allows to assess the methodology.

The general configuration investigated is a pair of circular diaphragms placed in a straight pipe. The downstream edge of each diaphragm has been chamfered. Figure 2 shows a sketch with main dimensions. Two cases have been selected to exhibit a resonance or not, depending on a single geometric parameter : the distance L between the diaphragms (Tab. 1).

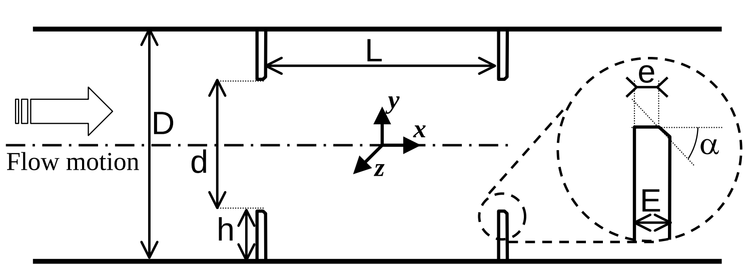

D	=	50 mm
d	=	28 mm
E	=	1.98 mm
e	=	0.9 mm
α	=	47.9^o
h	=	11 mm
L	=	**1D or 2D**

Figure 2. Generic sketch of investigated configuration for L1D and L2D cases

Case Name	**L1D**	**L2D**
Distance L between diaphragms	1D = 50mm	2D = 100mm
Aeroacoustic resonance	Strong tones	No tones
Bulk velocity	5 m/s	5 m/s

Table 1. Cases investigated experimentally

Both cases *L1D* & *L2D* are submitted to a constant flow of 5 m/s (bulk velocity). Since the tube upstream the section of interest is very long, the turbulent flow can be considered as fully developped. Acoustic conditions will be detailed in section IV.

III. Numerical approach

A. Large Eddy Simulations

LES have been has been carried out with *CERFACS*'s code *AVBP* that solves the full compressible 3D *Navier-Stokes* equations on hybrid grids. Even though the geometry is axisymmetric, all numerical simulations have performed on full 3D models. Subgrid stresses are described using dynamic Smagorinsky[13] model. The numerical scheme uses second-order (Lax-Wendroff[14] - LW) or third-order (Taylor-Galerkin[15] - TTGC) spatial and third-order explicit (Runge-Kutta) time accuracy.

The fully unstructured grids contains approximately 1M tetrahedra for case *L1D* and 1.5M tetrahedra for case *L2D*. As illustrated on Fig. 3, the meshes are significantly refined in the region of the upstream diaphragm's wake. Additionnal tests have been conducted on finer grids without showing significant differences.

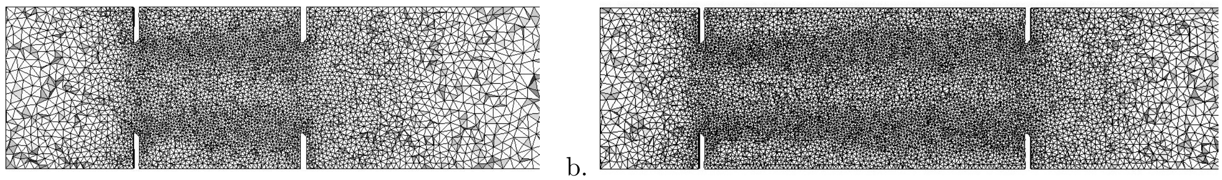

a. b.

Figure 3. Partial view of unstructured grids for a. case *L1D* and b. case *L2D*

B. Boundary conditions

The pipe adiabatic walls are handled using a wall function approach.[16] Besides, a classical Dirichlet no-slip treatment is applied on diaphragms walls. The inlet and outlet boundary condition treatment[17] is based on the NSCBC method.[18] Inlet velocity profile is driven towards a classical turbulent pipe flow.

From an acoustic point of view, inlet and outlet characteristic boundary conditions have been demonstrated to exhibit a low pass filter behaviour[19] with a cutoff frequency directly linked to the user-defined relaxation coefficient. It is consequently possible to adapt the boundary condition's impedance gradually to have fully, partially or almost non reflecting inlet/outlet. Table 2 summarizes the different numerical simulations performed within this study. Figure 4 presents, for partially reflecting case *L1D_TTGC_PR*, how the inlet/outlet impedance matches the measured reflection coefficients upstream and downstream the double diaphragm system.

	Simulation Name	**Scheme**	**Boundary Type**
L1D	*L1D_LW_NR*	Lax-Wendroff	Non-Reflecting
	L1D_LW_FR	Lax-Wendroff	Fully-Reflecting
	L1D_TTGC_PR	Taylor-Galerkin	Partially-Reflecting
	L1D_TTGC_NR	Taylor-Galerkin	Non-Reflecting
L2D	*L2D_LW_NR*	Lax-Wendroff	Non-Reflecting
	L2D_TTGC_NR	Taylor-Galerkin	Non-Reflecting

Table 2. Numerical simulations performed

IV. Experimental means

Along with the numerical simulations, detailed aeroacoustic measurements were performed in the silent and open *Matisse* test facility at the *Ecole Centrale of Lyon* (France). The experimental set-up (Fig. 5) allowed aerodynamic measurements (Laser Doppler Anemometry, noted LDA) and aeroacoustic measurements inside the duct (wall pressure fluctuations). The silent air supply is provided by a 2.2 kW centrifugal fan. In order to reduce the acoustic residual ambient noise due to the flow generation and to limit acoustic

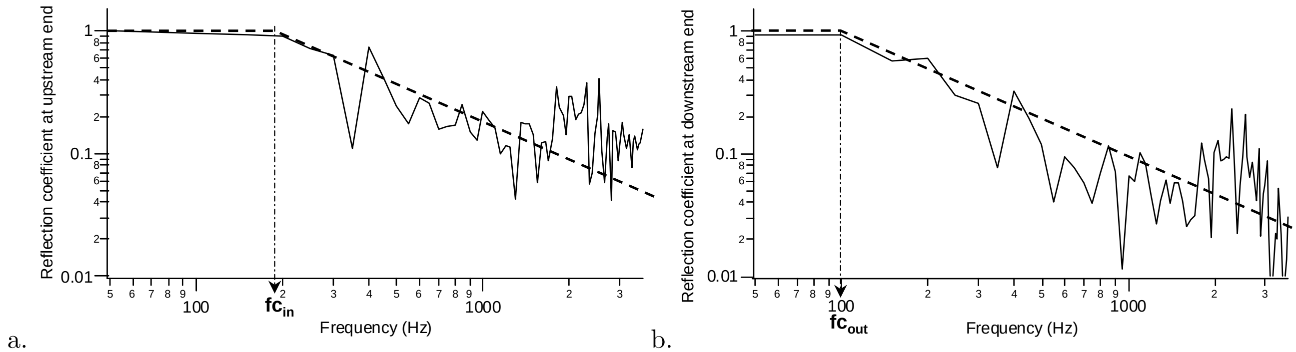

Figure 4. Reflection coefficients measured at a. upstream and b. downstream end of the setup (solid line) and boundary condition behaviour (dashed line) with cutoff frequency adjusted for partially reflecting inlet (fc_{in}) and outlet (fc_{out})

reflections, an acoustic treatment of the blower is realised. Moreover, a catenoidal pavilion was implanted at the end of the duct to limit upstream acoustic reflection. The test section (diameter 50 mm) is located more than 40 diameters after the convergent nozzle. Figure 4 presents the acoustics performances of the duct. The plane wave propagation hypothesis is validated between 500Hz and 2500Hz.

- From an aerodynamic point of view, mean and fluctuating flow measurements downstream and upstream the obstacle were measured thanks to the 2D LDA techniques (Fig. 6-a & b) along 11 profiles (Fig. 7).
- From an acoustic point of view, wall pressure fluctuations inside the duct were performed. B&K 1/4″ (ref.4939) microphones were used, flushed mounted without their protection grid (Fig. 6-c) at 5 different locations (Fig. 7).

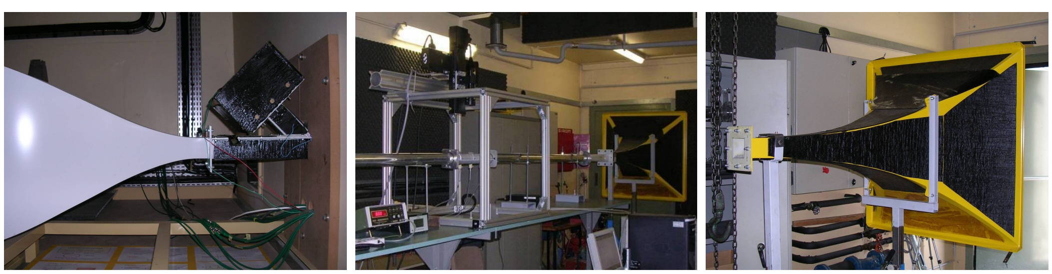

Figure 5. Views of the *Matisse* anechoic test facility

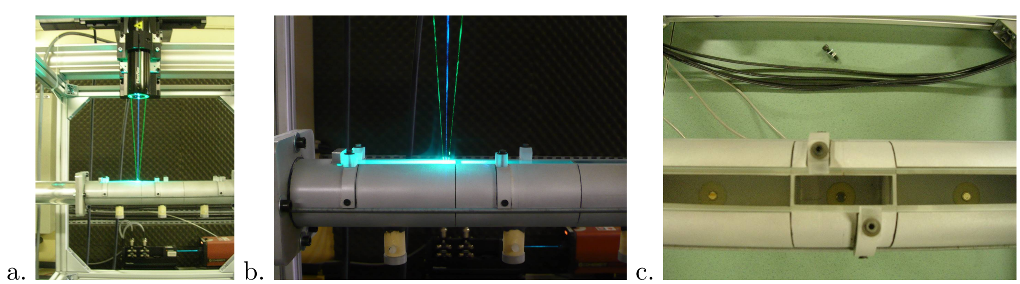

Figure 6. a. & b. : Views of the LDA set-up. c. : Flushed mounted microphones inside the duct

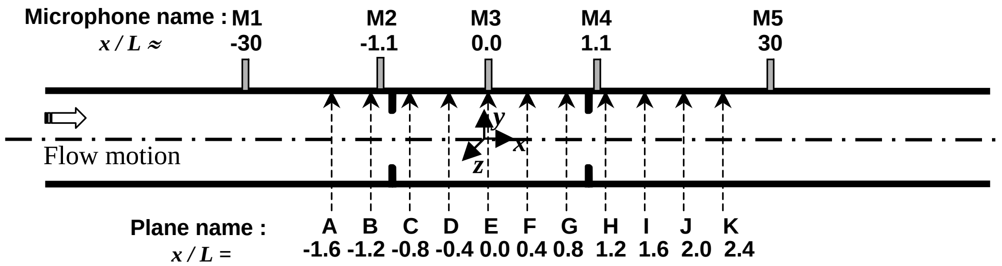

Figure 7. Location of measured velocity profiles and flush mounted microphones

V. Results and discussions

A. Case L1D

The physical mechanism identified by both experimental and numerical analysis is quite similar to the phenomenology introduced by *Rossiter*[20] on cavity flows : The turbulent eddies released at the edge of the upstream diaphragm are convected and impinge on the downstream diaphragm, generating strong acoustic waves. This feedback triggers a new set of eddies, therefore inducing a resonance loop.

The next subsections will describe the flow by looking at the evolution along the duct of axial mean and fluctuating velocities, using 11 profiles regularly distributed (see Fig. 7). Other components of the velocity yield the same conclusions and will not be displayed in this paper. From an acoustic point of view, classical spectral analysis (Spectral density from Fourier transform[21] with Hanning windowing) has been performed on wall pressure fluctuations. Due to the short signal obtained by LES (approximately 0.8s for each simulation) a compromise has been sought between on one hand the spectral resolution, and on the other the variance of the spectra. This point can be greatly improved in future studies by using advanced signal processing techniques.[22,23]

The aim of this chapter is to tackle step by step the following points :

1. By comparing cases *L1D_LW_NR* & *L1D_LW_FR*, evaluate the level of agreement between experiments and "standard" 2^{nd} order LES (LW scheme), and examine the effects of fully reflecting boundary conditon.
2. By comparing cases *L1D_TTGC_NR* & *L1D_LW_NR*, assess the potential improvement brought by 3^{rd} order TTGC scheme with respect to 2^{nd} order LW scheme.
3. By comparing cases *L1D_TTGC_NR* & *L1D_TTGC_PR*, try to match as best as possible the acoustic behaviour of BC and observe the impact on both aerodynamic profiles and pressure spectra.

Layout of Fig. 8 to Fig. 11 are kept the same to facilitate the reader's understanding. Table 3 summarizes the agreement achieved on peaks levels and frequencies for the different simulated cases.

Case L1D	**Peak 1**	**Peak 2**
Experiment	520 Hz / 108 dB	1050 Hz / 91 dB
L1D_LW_NR	511 Hz / 109 dB	1042 Hz / 85 dB
L1D_LW_FR	580 Hz / 101 dB	847 Hz / 95 dB
L1D_TTGC_NR	538 Hz / 98 dB	1078 Hz / 84 dB
L1D_TTGC_PR	532 Hz / 100 dB	1056 Hz / 84 dB

Table 3. Resonance frequencies and peak level obtained on microphone M3 for case *L1D*

1. Level of agreement & spurious effects of reflecting BC

Figure 8 presents the evolution of axial mean velocity (Fig. 8-a) and RMS fluctuations Fig. 8-b) on the 11 profiles described on Fig. 7. The toroidal recirculation zone between the diaphragms is well captured. The development of turbulent eddies between the diaphragms is clearly visible with the increase of U_{RMS} in the wake of the upstream diaphragm. When LW scheme is used, the agreement between experimental measurements and numerical results is reasonnable on mean velocity profiles, and average on RMS fields. The RMS peak in the vicinity of the upstream diaphragm (Plane C) is clearly underestimated and the fluctuations close to the axis overestimated (Planes E to H). Surprisingly, the differences in aerodynamic fields between reflecting and non reflecting BC are limited. Only velocity fluctuations along centerline are slightly larger for case *L1D_LW_FR*.

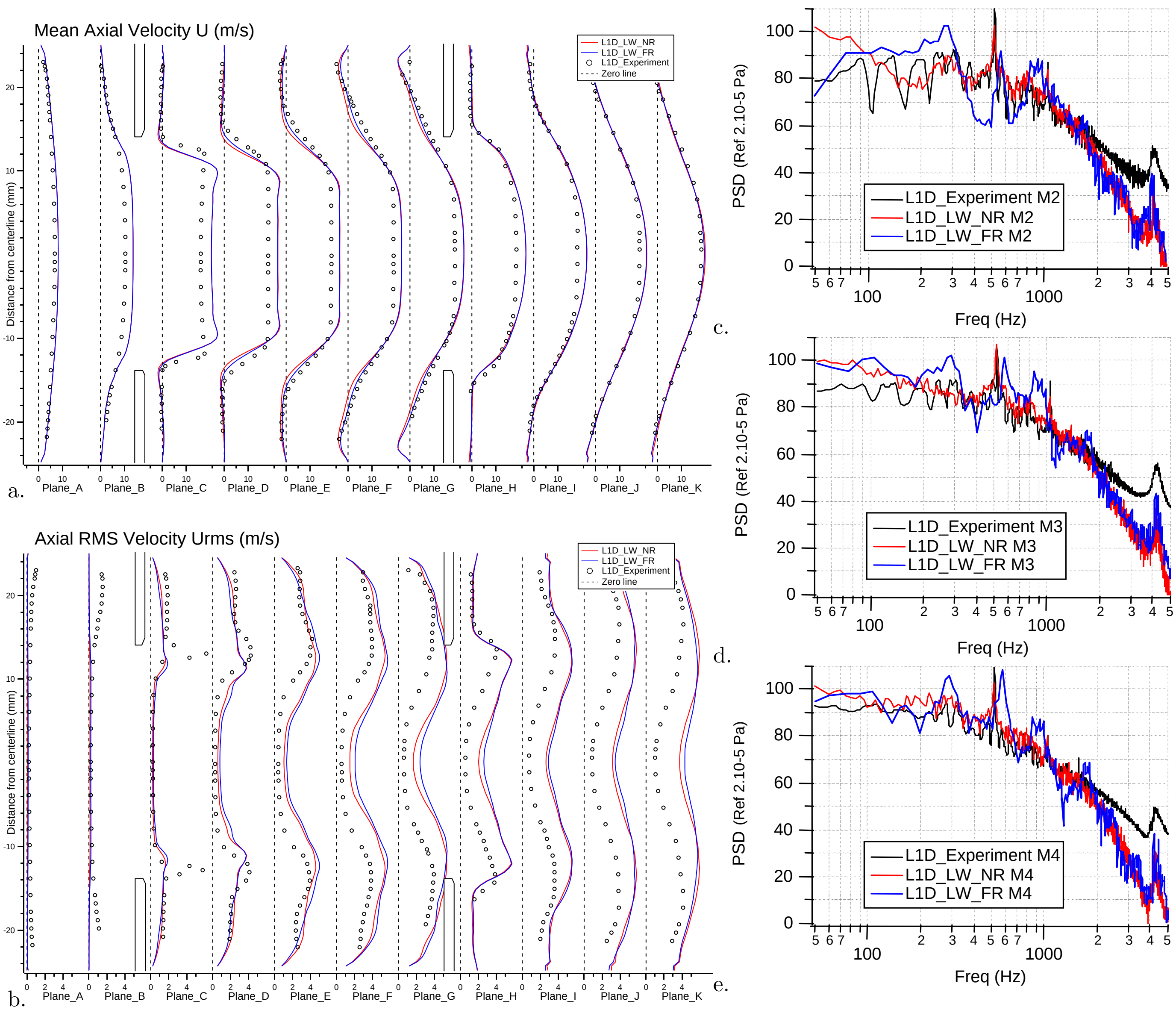

Figure 8. Comparison of a. mean, and b. RMS axial velocity profiles on L1D case. Comparison of wall pressure spectra from microphones c. M2, d. M3 and e. M4. Symbols : Experiment; Red line : *L1D_LW_NR*; Blue line : *L1D_LW_FR*; Dashed line : zero line

Case *L1D_LW_NR* shows quite good agreement on wall pressure spectra (Fig. 8-c,d,e). Peaks frequency and amplitude are captured properly. However, the spectral decay is not well predicted, and the mismatch becomes larger and larger over 2000 Hz. With case *L1D_LW_FR*, spurious peaks are appearing : Acoustic energy is partially redistributed in eigen modes of the computationnal domain (around 280Hz, 580Hz, 855Hz and 1800Hz), which is highly non-physical. Such a fundamental difference was visible neither on aerodynamic mean nor RMS fields.

2. Improvements brought by TTGC scheme

Switching from 2^{nd} order LW scheme to 3^{rd} order TTGC scheme yields changes in velocity profiles. With TTGC, the mean velocities (Fig. 9-a) are slightly better computed in the shear flows regions. A much more important improvement is observed on RMS profiles (Fig. 9-b) : the RMS peak in the vicinity of the upstream diaphragm is qualitatively captured, and the right level of fluctuations is caught up in the impingement zone, close to downstream diaphragm.

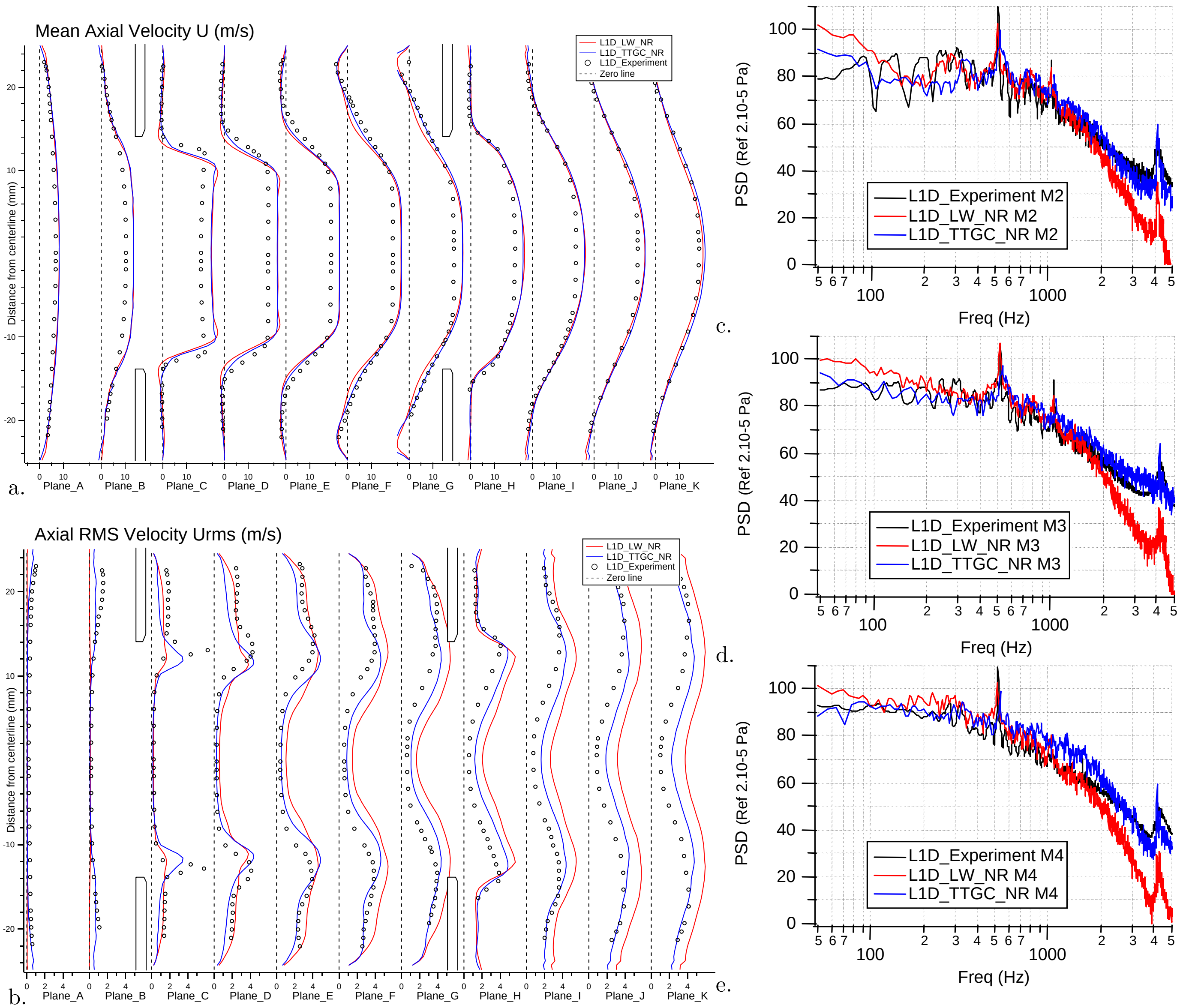

Figure 9. Comparison of a. mean, and b. RMS axial velocity profiles on L1D case. Comparison of wall pressure spectra from microphones c. M2, d. M3 and e. M4. Black symbols : Experiment; Red line : *L1D_LW_NR*; Blue line : *L1D_TTGC_NR*; Dashed line : zero line

The effect of 3^{rd} order numerical scheme is also noticeable on pressure spectra (Fig. 9-c,d,e). Although the agreement on peaks is left unchanged, TTGC clearly improves the spectral decay of broadband noise over 2000Hz until the duct cuttoff frequency (5000Hz). Dissipation and dispersion of LW 2^{nd} order is probably to blame on the incorrect prediction of decay slope.

3. Fine tuning of boundary condition's acoustic behaviour

When the most appropriate boundary condition's impedance is selected (case *L1D_TTGC_PR*), the change observed is somehow very limited with respect to non reflecting BC (case *L1D_TTGC_NR*). Mean velocity profiles (Fig. 10-a) are exactly the same. RMS fluctuations (Fig. 10-b) are very slightly improved in the recirculation zones between the diaphragms.

Pressure spectra (Fig. 10-c,d,e) are as well very similar between cases case *L1D_TTGC_NR* and *L1D_TTGC_PR*. Spectral densities seem to be slightly higher at very low frequency (100Hz to 200Hz), but whithout any other consequences on both peaks and decay of broadband noise.

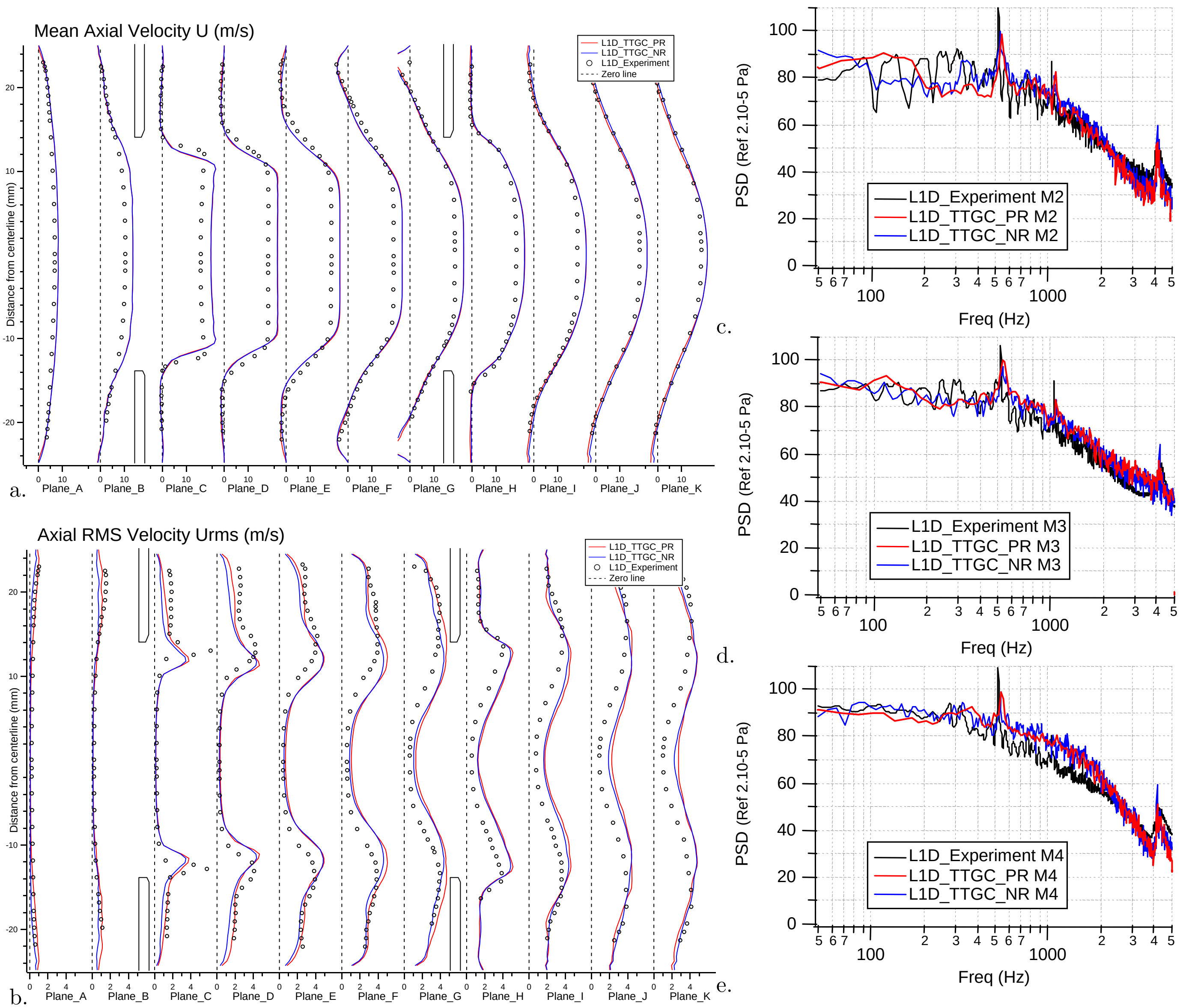

Figure 10. Comparison of a. mean, and b. RMS axial velocity profiles on L1D case. Comparison of wall pressure spectra from microphones c. M2, d. M3 and e. M4. Black symbols : Experiment; Red line : *L1D_TTGC_PR*; Blue line : *L1D_TTGC_NR*; Dashed line : zero line

The outcome of this subsection is that an accurate scheme and appropriate non reflecting BC should be employed to capture such phenomena. For the case considered, the flow does not appear to highly sensitive to BC's impedance, but one should take special care wih this point on other cases where bifurcation in the physical mechanism might occur.

B. Case L2D

Experimental measurements shows that for case *L2D*, the tonal noise disappears and only broadband content remains. By comparing *L2D* (Fig. 11) with respect to previous *L1D* profiles (Fig. 9) some elements may explain this trend : With the increased distance *L*, the convective time between the diaphragms is increased as well, allowing turbulent eddies to develop, mix and vanish longer. The typical length scale of eddies is therefore larger when impinging the downstream diaphragm. Figure 11-a,b shows that both mean and RMS axial velocity profiles are much smoother at plane G. The recirculation is also much smaller for case *L2D*. Surpisingly, the level of velocity fluctuations in the impingement zone (of the order of 4m/s) si not significantly lower for case *L2D* than for case *L1D*; only the shape of the profile seems to be impacted. Moreover, the same conclusions related to the benefits of accurate numerical scheme can be drawn from the differences between simulations *L2D_LW_NR* and *L2D_TTGC_NR*.

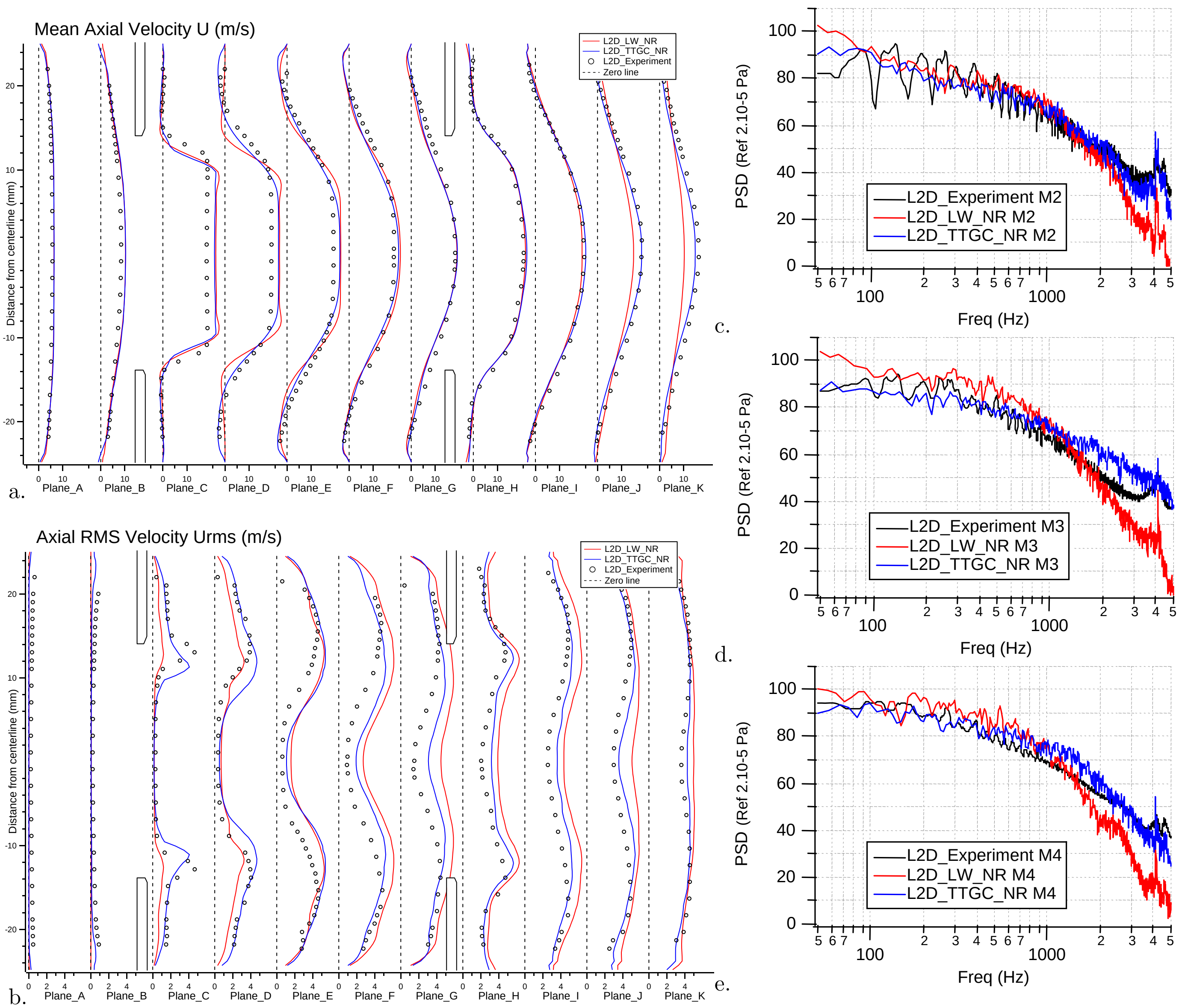

Figure 11. Comparison of a. mean, and b. RMS axial velocity profiles on L2D case. Comparison of wall pressure spectra from microphones c. M2, d. M3 and e. M4. Black symbols : Experiment; Red line : *L2D_LW_NR*; Blue line : *L2D_TTGC_NR*; Dashed line : zero line

From an acoustic point of view, the tonal peaks have completely faded out on pressure spectra (Fig. 11-c,d,e). This trend is captured by LES, which seems to confirm the potential of this method. The overall shape of the spectra is well predicted by TTGC scheme on all frequency range, whereas LW scheme displays the same lacks on high frequencies.

VI. Conclusion

This paper presents a joint experimental and numerical effort to study the resonance that occurs in a double diaphragm system, with all non linear phenomena involved. The potential of unstructured LES on this kind of configuration has clearly been evidenced. Even for a reasonable computational effort, capturing trends between designs is possible. Some golden rules seem to come out of this study :

- The leap between 2^{nd} order and 3^{rd} order numerical schemes is significant, yielding much better results in terms of both aerodynamic and acoustic representation of the flow.
- Validation only based on velocity profiles, even on RMS fluctuations is insufficient to ensure acoustic predictions. Non-reflecting boundary conditions are mandatory to achieve a proper spectral representation.
- Even if fine tuning of boundary conditions' impedance was unnecessary here, this conclusion should not be generalized. Acoustic behaviour of computational domains' boundaries should still be handled carefully.

More generally, this study opens up perspectives of numerical evaluation of aeroacoustic sources in various complex-geometry parts. Together with an acoustic network code, LES could yield promising results towards quieter air-conditioning systems.

References

[1] Bogey, C. and Bailly, C., "investigations of subsonic jet noise using LES : Mach and reynolds number effects," *AIAA paper 2004-3023*, 2004.

[2] Bodony, D. J. and Lele, S. K., "On using large-eddy simulation for the prediction of noise from cold and heated turbulent jets," *Phys. Fluids* , Vol. 085103, 2005.

[3] Bodony, D. J. and Lele, S. K., "Spatial Scale Decomposition of Shear Layer Turbulence and the Sound Sources Associated with the Missing Scales in a Large-Eddy Simulation," *8th AIAA/CEAS Aeroacoustics Conference, AIAA paper 2002-2454*, 2002.

[4] Ewert, R., Schroder, W., M., M., and A., E.-A. W., "LES as a Basis to Determine Sound Emission," *40th AIAA Aerospace Sciences Meeting & Exhibit, AIAA paper 2002-0568*, 2002.

[5] Terracol, M., Manoha, E., Herrero, C., Labourasse, E., Redonnet, S., and Sagaut, P., "Hybrid methods for airframe noise numerical prediction," *Theor. Comput. Fluid Dyn.*, Vol. 19, 2005, pp. 197–227.

[6] Imamura, T., Enomoto, S., and Yamamoto, K., "3D Unsteady Flow Computations in a Slat Cove Using Large Eddy Simulation," *12th AIAA/CEAS Aeroacoustics Conference, AIAA paper 2006-2668*, 2006.

[7] Lele, S., "Compact finite difference schemes with spectral like resolution," *J. Comput. Phys.* , Vol. 103, 1992, pp. 16–42.

[8] Bogey, C. and Bailly, C., "A family of low dispersive and low dissipative explicit schemes for noise computation," *J. Comput. Phys.* , Vol. 194, No. 1, 2004, pp. 194–214.

[9] Birbaud, A. L., Ducruix, S., Durox, D., and Candel, S., "Dynamics of Free Jets Modulated by Plane Acoustic Waves : Part 2. Numerical Simulations," *12th AIAA/CEAS Aeroacoustics Conference, AIAA paper 2006-2670*, 2006.

[10] Mathey, F., Morin, O., Caruelle, B., and Debatin, K., "Simulation of Aero-acoustic Sources in Aircraft Climate Control Systems," *12th AIAA/CEAS Aeroacoustics Conference*, No. AIAA 2006-2493, 2006.

[11] Mendonca, F., Caruelle, B., and Debatin, K., "Aeroacoustic Simulation of Double Diaphragm Orifices in an Aircraft Climate Control System," *11th AIAA/CEAS Aeroacoustics Conference*, No. AIAA 2005-2917, 2005.

[12] Belanger, A., Meskine, M., Caruelle, B., and Debatin, K., "Aero-acoustic Simulation of a Double Diaphragm Using Lattice Boltzmann Method," *11th AIAA/CEAS Aeroacoustics Conference*, No. AIAA 2005-2917, 2005.

[13] Germano, M., Piomelli, U., Moin, P., and Cabot, W., "A dynamic subgrid-scale eddy viscosity model," *Phys. Fluids* , Vol. 3, No. 7, 1991, pp. 1760–1765.

[14] Lax, P. and Wendroff, B., "Systems of conservation laws," *Commun. Pure and Appl. Math.*, Vol. 13, 1960, pp. 217–37.

[15] Colin, O. and Rudgyard, M., "Development of high-order Taylor-Galerkin schemes for unsteady calculations," *J. Comput. Phys.* , Vol. 162, No. 2, 2000, pp. 338–371.

[16] Schmitt, P., Schuermans, B., Geigle, K., and Poinsot, T., "Large-eddy simulation and experimental study of heat transfer, nitric oxide emissions and combustion instability in a swirled turbulent high pressure burner," *J. Fluid Mech.* , Vol. 570, 2007, pp. 17–46.

[17] Moureau, V., Lartigue, G., Sommerer, Y., Angelberger, C., Colin, O., and Poinsot, T., "Numerical methods for unsteady compressible multi component reacting flows on fixed and moving grids," *J. Comput. Phys.* , Vol. 202, 2005, pp. 710–736.

[18] Poinsot, T. and Lele, S., "Boundary conditions for direct simulations of compressible viscous flows," *J. Comput. Phys.* , Vol. 101, No. 1, 1992, pp. 104–129.

[19]Selle, L., Nicoud, F., and Poinsot, T., "The actual impedance of non-reflecting boundary conditions: implications for the computation of resonators," *AIAA Journal* , Vol. 42, No. 5, 2004, pp. 958–964.

[20]Rossiter, J., "Wind-tunnel experiments on the flow over rectangular cavities at subsonic and transonic speeds," *Aeronautical Research Council Reports and Memoranda, Technical Report*, Vol. 3438, 1964.

[21]Welch, P. D., "The use of FFT for the estimation of power spectra," *IEEE transactions on audio and electroacoustics*, Vol. 15, No. 2, 1967.

[22]Burg, J. P., "Maximum entropy spectral analysis," *proc. 37th ann. internat. meeting, soc. of Explor. Geophys.*, 1967.

[23]Capon, J., "High resolution frequency-wavenumber spectrum analysis," *Proceedings of IEEE*, Vol. 57, 1969, pp. 1408–1418.

Acknowledgments

The help of *Philippe BOUSQUET*, from Airbus acoustic laboratory (EVTXGA) at several key stages of this study is greatly acknowledged.

All numerical simulations have been conducted on CERFACS' *IBM BladeCenter* and *CRAY* XD_1 supercomputers.